ELSEVIER

Earth and Planetary Science Letters 208 (2003) 271–278

EPSL

www.elsevier.com/locate/epsl

The breakdown of diopside to Ca-rich majorite and glass in a shocked H chondrite

Naotaka Tomioka [a,*], Makoto Kimura [b]

[a] *Department of Earth and Planetary Sciences, Faculty of Science, Kobe University, Kobe 657-8501, Japan*
[b] *Faculty of Science, Ibaraki University, Mito 310-8512, Japan*

Received 17 July 2002; received in revised form 24 October 2002; accepted 17 January 2003

Abstract

Fine-grained assemblages of majorite and glassy grains are for the first time identified in a shock-induced melt vein in an H chondritic meteorite. The bulk chemical composition of these aggregates is similar to that of diopside $CaMgSi_2O_6$ in the host rock. Both majorite and glassy grains are Ca-rich and their formulae can be approximated as $(Mg_{0.65}Fe_{0.09}Ca_{0.26})SiO_3$ and $(Mg_{0.23}Fe_{0.05}Ca_{0.72})SiO_3$, respectively. These Ca-rich assemblages are dissociation products of the host diopside and were produced at ~18–24 GPa by a shock event. The $CaSiO_3$-rich glass is inferred to have crystallized in a perovskite structure, but was vitrified during the pressure release.

Keywords: shock event; H chondrite; diopside; majorite; perovskite

1. Introduction

Olivine, high-Ca pyroxene, low-Ca pyroxene, and plagioclase are the major constituent minerals of chondritic meteorites. Ultrahigh-pressure polymorphs of olivine (wadsleyite, ringwoodite), low-Ca pyroxene (majorite, akimotoite, and perovskite-phase), and plagioclase (hollandite-phase) have previously been discovered in shock-induced melt veins in ordinary chondrites by analytical transmission electron microscopy (ATEM), X-ray diffraction, and Raman spectroscopy [1–8]. Ultrahigh-pressure minerals not only record the pressure–temperature histories of the impact events in chondrite parent bodies, but also provide clues to understanding the structure and dynamics of the deep Earth (e.g. [9–11]). As for high-Ca pyroxene, Malavergne et al. first discovered majorite with augite composition in a shocked Martian meteorite [12]. However, high-pressure phase transition of high-Ca pyroxene has not been discovered in ordinary chondrites, probably due to the relatively low abundance of high-Ca pyroxene among major silicates.

High-pressure experiments have demonstrated that diopside $CaMgSi_2O_6$, which is one of the Ca-rich end-members of the pyroxene quadrilateral, dissociates at high temperatures with increasing pressure into the assemblages of high-pressure phases including $MgSiO_3$-garnet (majorite)+ $CaSiO_3$-perovskite, $MgSiO_3$-ilmenite (akimotoite)

* Corresponding author. Tel.: +81-78-803-5748.
E-mail address: nao@kobe-u.ac.jp (N. Tomioka).

0012-821X/03/$ – see front matter
doi:10.1016/S0012-821X(03)00049-9

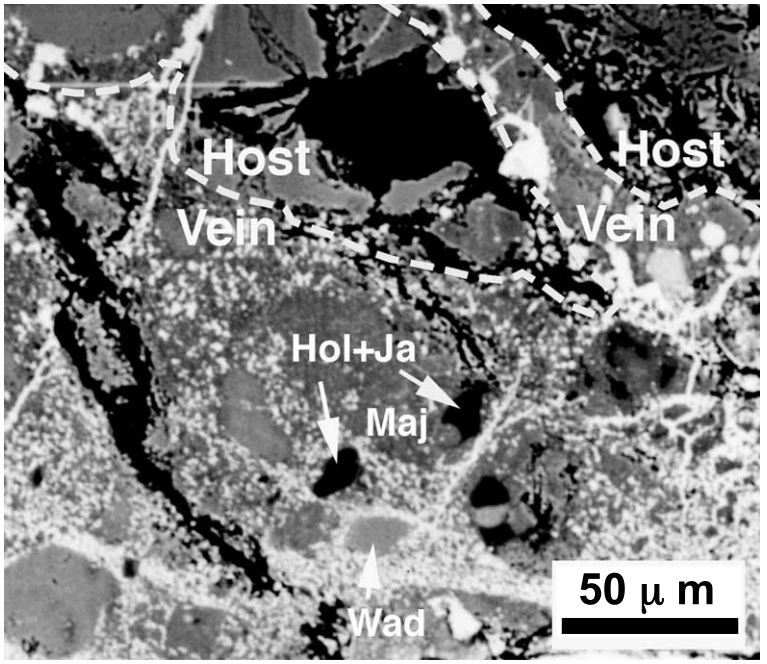

Fig. 1. Backscattered electron image of a shock-induced melt vein in the Y75100 chondrite. The shock vein contains rounded to irregular fragments of the host chondritic rock. The fragments are entrapped into a fine-grained matrix of silicate, metal and troilite, and transformed into high-pressure phases, such as hollandite (Hol), majorite (Maj), jadeite (Ja), and wadsleyite (Wad) [15].

+$CaSiO_3$-perovskite, and $MgSiO_3$-perovskite+$CaSiO_3$-perovskite [13]. In this study, we describe the first evidence for high-pressure transformation of diopside into Ca-rich majorite and perovskite in a shock-induced melt vein in an H chondrite.

2. ATEM observations

We examined the Y75100 meteorite collected in Antarctica, which is an ordinary chondrite classified as an H6, mainly consisting of olivine, low-Ca pyroxene, high-Ca pyroxene, plagioclase, kamacite and troilite. It is highly shocked and has the highest shock stage (S6) of a scheme of six stages (S1–S6) of shock classified by Stöffler et al. [14]. It contains shock-induced melt veins of less than 1 mm in thickness. In these veins, rounded to irregular fragments ($\sim$10–100 μm in size) of the host minerals are enclosed in fine-grained (<5 μm) mineral aggregates [15]. We used ATEM to characterize the microstructures of the shock veins by conventional TEM imaging techniques, to identify mineral phases on the basis of quantitative energy-dispersive X-ray spectroscopy (EDS) and selected area electron diffraction (SAED).

Specimens for the ATEM observations were removed from a polished thin section and prepared as thin foil by Ar ion bombardment at 3 kV and 0.5 mA. In order to minimize the structural damage by Ar^+ beam heating, ion milling was done using a liquid-nitrogen-cooled specimen holder. The TEM observations were conducted using a JEOL 2010 instrument with an accelerating voltage of 200 kV and equipped with the Noran Voyager EDS system. *k*-Factors for the major elements were determined using standards of natural olivine, pyroxene and feldspar. The procedure for the thickness corrections of the *k*-factor is described by Fujino et al. [16].

Laser Raman spectroscopy clarified that shock veins contained polycrystalline fragments of high-pressure minerals, such as ringwoodite, wadsleyite (Mg_2SiO_4 polymorphs), akimotoite ($MgSiO_3$ polymorph), hollandite-phase ($NaAlSi_3O_8$ polymorph) and jadeite (Fig. 1) [15]. The fine-grained

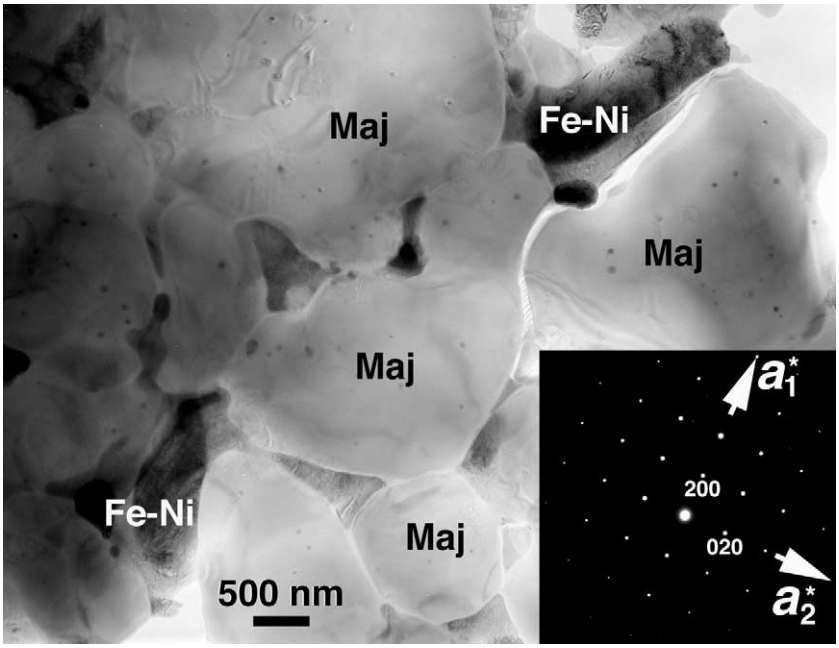

Fig. 2. Transmission electron micrograph of a shock vein in Y75100. Low-Ca majorite (Maj) coexisting with Fe–Ni alloy (Fe–Ni). Low-Ca majorite occurs in coarser grains (1–3 μm) than Ca-rich majorite. SAED pattern taken from low-Ca majorite in the center of the micrograph is presented in the inset.

Table 1
Representative ATEM microanalyses of minerals in the shock vein in the Y75100 chondrite

	Low-Ca majorite	Ca-rich majorite	Ca-rich glass	Ca-rich aggregate
Oxide (wt%)				
Na_2O	0.58	1.40	1.09	0.75
MgO	28.77	21.87	7.29	17.04
Al_2O_3	2.86	0.74	2.47	0.44
SiO_2	54.96	56.41	51.88	54.07
K_2O	0.03	0.00	0.25	0.09
CaO	2.83	12.06	32.24	20.96
TiO_2	0.13	0.12	1.03	0.39
Cr_2O_3	0.81	0.82	0.61	0.61
MnO	0.52	0.52	0.30	0.21
FeO	8.52	6.07	2.85	5.43
Formula (O = 12)				
Na	0.08	0.19	0.16	0.10
Mg	3.02	2.33	0.82	1.86
Al	0.24	0.06	0.22	0.04
Si	3.88	4.04	3.90	3.97
K	0.00	0.00	0.02	0.01
Ca	0.21	0.93	2.60	1.65
Ti	0.01	0.01	0.06	0.02
Cr	0.05	0.05	0.03	0.04
Mn	0.03	0.03	0.02	0.01
Fe	0.50	0.36	0.18	0.33
Total cations	8.02	8.00	8.01	8.03

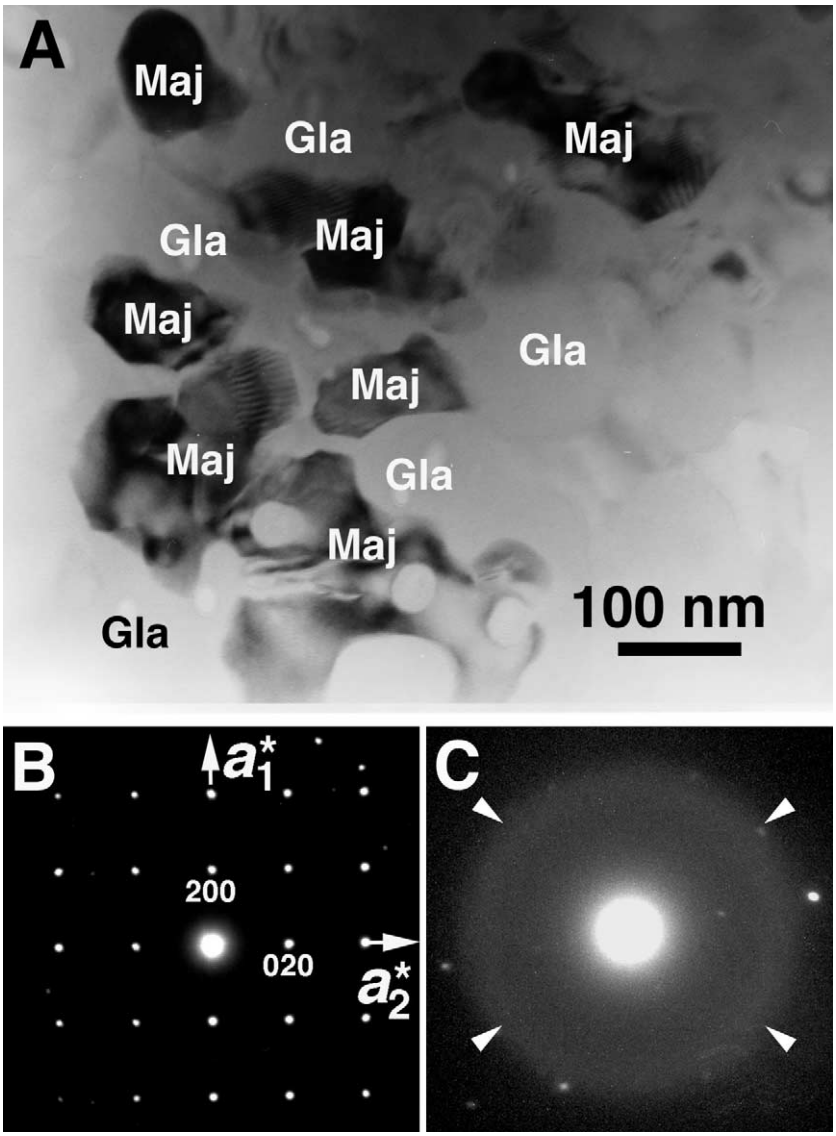

Fig. 3. Transmission electron micrographs of the assemblage of Ca-rich majorite (Maj) and Ca-rich glass (Gla). (A) Both phases occur as fine grains (100–400 nm). The small spots in majorite grains are the damage caused by the electron beam during the EDS analysis. (B) SAED pattern of Ca-rich majorite along [001] zone axis. (C) The diffuse electron scattering from Ca-rich glass. Some diffraction spots from neighboring Ca-rich majorite crystals overlap, because the Ca-rich grains are smaller than the diameter of the selected area aperture.

matrix of the veins is dominated by majorite or low-Ca pyroxene [15]. These minerals indicate the generation of high pressures and high temperatures by an impact event on the parent body of the chondrite.

In the area examined by ATEM, low-Ca majorite forms relatively large crystals ($\sim$1–3 μm), and their interstices are filled by opaque minerals, such as kamacite and troilite (Fig. 2). Fe-rich inclusions are often enclosed as tiny blebs ($< \sim$100 nm) inside the majorite crystals. These occurrences resemble that of majorite in the shock veins in the Sixiangkou (L6) chondrite [17]. Low-Ca majorite crystallized from shock-induced melt,

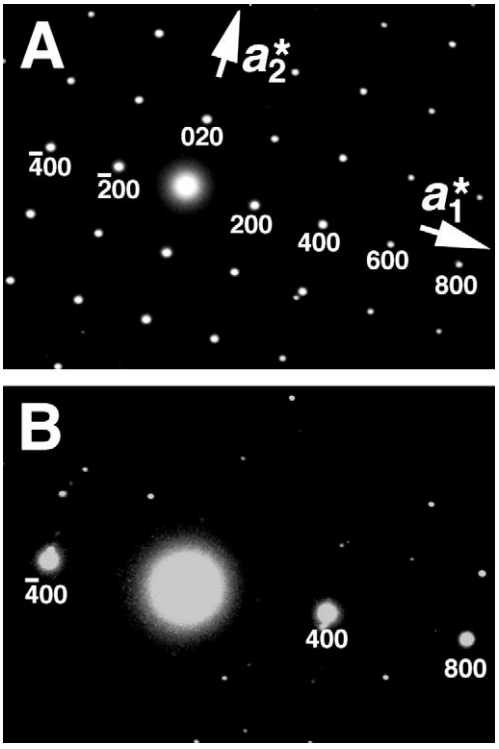

Fig. 4. SAED patterns of cubic Ca-rich majorite with space group $Ia\bar{3}d$. (A) A diffraction pattern along the [001] zone axis. The diffraction spots of (200), (600), ($\bar{2}$00) planes are due to multiple diffraction. (B) SAED pattern of Ca-rich majorite by tilting from the orientation of panel A. The spots from multiple diffraction ({2n 0 0}: n = odd) are absent. Some extra spots come from the neighboring Ca-rich majorite crystals.

which is supported by the incorporation of Na and Al in these majorites [15,17].

Very fine-grained assemblages with crystals several μm in size are found in one of the shock veins (Fig. 3A). It is adjacent to an aggregate of $NaAlSi_3O_8$-hollandite or assemblages of majorite+FeS+FeNi. Individual grains are 100–400 nm in diameter. These aggregates consist of two kinds of grains. SAED patterns taken from the crystalline phase are consistent with a majorite (garnet) structure (Fig. 3B). The systematic absences of {2n 0 0} reflections of majorite with n = odd suggest its space group is $Ia\bar{3}d$ (cubic), but not a tetragonal symmetry with space group $I4_1/a$ (Fig. 4; see [18]). Quantitative chemical analyses by ATEM revealed that it has a pyroxene stoichiometry, with the composition (Ca,Mg,Fe)SiO_3 (Table 1). Its average composition is $En_{65}Fs_9Wo_{26}$ (Fig. 5). This majorite is enriched in Ca and poor in Al in comparison with the low-Ca majorites crystallized from melt in the matrix of the shock veins. Both low-Ca and Ca-rich majorites have neither modulated structure nor twinning, which are reported in synthetic majorite with a tetragonal ($I4_1/a$) symmetry [18–21].

Another phase coexisting with Ca-rich majorite shows a diffuse ring pattern and does not show diffraction contrast in any specimen tilt. Therefore, it is amorphous (Fig. 3C). Nevertheless, it also has pyroxene stoichiometry $En_{23}Fs_5Wo_{72}$ (Table 1, Fig. 5). We also analyzed Ca-rich majorite plus glass aggregates using ATEM with a broader electron beam (~1–2 μm in diameter). The average composition of these aggregates is $En_{49}Fs_8Wo_{43}$. This composition is similar, though not identical, to the chemistry obtained by electron microprobe analyses of diopside ($En_{47}Fs_6Wo_{47}$) in the host rock. The grain sizes of Ca-rich majorite and glass are not small enough (100–400 nm in size) to allow the precise bulk compositions with respect to the electron beam size (~1–2 μm in diameter) in ATEM analyses. Therefore, slight differences in composition

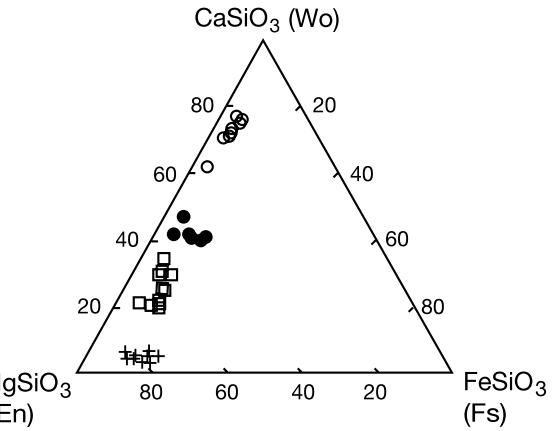

Fig. 5. Chemical compositions of various phases obtained by ATEM and plotted in a ternary $MgSiO_3$–$FeSiO_3$–$CaSiO_3$ diagram. Crosses are low-Ca majorite, open circles are Ca-rich glass, and open squares are Ca-rich majorite. Filled circles are the compositions of Ca-rich majorite and glass assemblage analyzed by a broad electron beam (~1–2 μm in diameter).

between Ca-rich aggregates and host diopside apparently result from this analytical uncertainty.

3. Discussion

Significantly Ca-rich majorite was first reported in the Shergotty Martian meteorite [12]. In that occurrence, it is also associated with amorphous material that is highly enriched in Si and Al. The chemical composition of this majorite is almost identical to augite ($En_{46}Fs_{29}Wo_{25}$) that is commonly observed in the host rock. This majorite formed by a solid-state reaction from augite [12]. In Y75100, Ca-rich majorite and glass have quite different compositions, especially with respect to Ca of the host diopside, but the bulk composition of their aggregates is nearly the same (Fig. 5, Table 1). This suggests that Ca-rich majorite and glass are dissociation products of diopside in a solid-state reaction.

There is also the possibility that Ca-rich majorite and glass formed from shock-induced melt. However, the Al content in the Ca-rich majorite is low (less than 1 wt%) as in diopside ($\sim$0.6 wt%), compared with low-Ca majorite (up to $\sim$4 wt %) as a liquidus phase. If the Ca-rich majorite also crystallized from melt, it would have a higher content of Al_2O_3, mainly derived from melted plagioclase of the host rock. In addition, Ca-rich assemblages do not contain Fe-rich interstitial phases, although they are in direct contact with low-Ca majorite+FeS+FeNi assemblages, and liquidus majorite abundantly contains such phases. Therefore, the crystallization of Ca-rich assemblages from a chondritic or an isolated diopside melt is not plausible. Alternatively, this assemblage is more likely the dissociation product of diopside.

Ca-rich majorite and glass considered in this study have a granular texture. In the dissociation process in pyroxene, fine symplectitic intergrowths are expected, because rates of cation diffusion in pyroxene are much more sluggish in comparison with those in olivine [22–24]. However, Ca-rich assemblages were heated by surrounding hot shock melt (its temperature is greater than $\sim$1900°C as described below). Rates of cation diffusion in diopside could be large enough to produce granular grains rather than symplectitic intergrowths, if host diopside in Y75100 dissociated at temperatures close to the solidus temperature of the bulk chondrite.

Ca-rich glass is complementary in composition to Ca-rich majorite in the breakdown products of diopside under ultrahigh pressure. This glass is especially rich in $CaSiO_3$ component. According to high-pressure experiments in $CaSiO_3$, a phase with the perovskite structure is stable above $\sim$12 GPa and $\sim$1000°C, but it retrogressively transforms into glass on the release of pressure [25,26]. Therefore, Ca-rich glass in Y75100 could have initially formed as Ca-rich perovskite and subsequently vitrified during decompression. Its granular shape also suggests that Ca-rich glass was originally crystals and did not form by quenching from the residual melt following the crystallization of Ca-rich majorite.

According to Gasparik [27,28], the solubility of the $CaSiO_3$ component in $MgSiO_3$ majorite is at most $\sim$14 mol% in the pressure range $\sim$16–22 GPa above 1650°C in the system $MgSiO_3$–$CaSiO_3$. Gasparik also reported that the structure unknown 'CM-phase' with $En_{\sim 60}Wo_{\sim 40}$ composition formed in the pressure range $\sim$16–18 GPa [27]. This CM-phase was further deduced to have a majorite structure resulting from immiscibility in majorite solid solution [28]. Ca-rich majorite in this study has a chemical composition ($En_{65}Fs_9Wo_{26}$) close to the system enstatite–diopside, but has an intermediate $CaSiO_3$ content between that in low-Ca majorite and that in the CM-phase noted in Gasparik's phase diagram. In the present study, the formation of Ca-rich majorite is due to the metastable reaction or is due to the fact that some Fe content may significantly decrease the immiscibility gap between the low-Ca majorite and the CM-phase (assumed as Ca-rich majorite). Further phase equilibria studies of Fe-bearing diopside are necessary to reveal the solubility of $CaSiO_3$ in majorite and the nature of the CM-phase.

The occurrence of high-pressure phases provides some constraints on pressure and temperature during a shock event. Majorites, both low-Ca and Ca-rich in Y75100, have a cubic symmetry.

This is consistent with previous studies on Al-poor majorite in ordinary chondrites [29,30]. The tetragonal distortion from cubic majorite is thought to be caused by cation ordering in its octahedral sites with decreasing temperature [31]. In shocked chondrites, the cubic symmetry of Al-poor majorite was preserved due to a very high cooling rate (higher than $\sim 10^3$°C/s), which prevented cation ordering [18]. The cooling rate of shock veins could be much faster than previously deduced rates based on shock experiments [14]. Langenhorst and Poirier [32] estimated the solidification time of shock veins by thermal modeling. They concluded that the contribution of adiabatic cooling is almost negligible during quenching of shock veins. Thus, the very high cooling rate deduced by the present study would be mainly caused by the thermal conduction before the decompression process.

The assemblage of majorite plus Ca-rich perovskite (now glass) is stable at ~18–24 GPa at ~1100–2100°C based on the phase diagram of $CaMgSi_2O_6$ [13]. The solidus temperature of the bulk chondrite is ~1900°C in this pressure range [33]. Above this temperature, diopside chemically reacts in a melting process with the surrounding minerals. Hence, the condition for the dissociation should not exceed ~1900°C and ~24 GPa. This is consistent with the formation of ringwoodite, akimotoite and $NaAlSi_3O_8$-hollandite found as polycrystalline aggregates in the shock veins in Y75100. According to the melting experiments of the Allende carbonaceous (CV3) chondrite, low-Ca aluminous majorite is a liquidus phase between 14 and 26 GPa [33]. In the H chondrite, FeO content is significantly lower than that in the CV3 chondrites. Therefore, the liquidus temperature and the phase relations in the H chondrites at high pressure and temperature are not exactly the same as those in Allende. However, such experimental results indicate that the crystallization pressure of the bulk chondrite melt is tentatively between 14 and 26 GPa assuming that equilibrium crystallization of low-Ca majorite occurred in Y75100. Although high-pressure minerals are not common in most H chondrites [15], the parent body of the H chondrite would have locally experienced similar shock pressures as those in some shocked L chondrites such as Tenham and Sixiangkou, also yielding aluminous majorite from a shock melt [17,34].

Acknowledgements

We acknowledge K. Tomeoka for discussions and D. Ito, K. Kiriyama and I. Ohnishi for their technical assistance. We also thank P. Buchanan for improving the manuscript, and Thomas Sharp and an anonymous reviewer for their careful reviews. The sample was supplied by the National Institute of Polar Research (NIPR). This work was supported by the Grant-in-Aid for Scientific Research from the Ministry of Education, Science and Culture (No. 12440149 and No. 13874060 to N.T., No. 09640562 and No. 11640473 to M.K.).*[BW]*

References

[1] B. Mason, J. Nelen, J.S. White, Olivine-garnet transformation in a meteorite, Science 160 (1968) 66–67.
[2] R.A. Binns, R.J. Davis, S.J.B. Reed, Ringwoodite, natural $(Mg, Fe)_2SiO_4$ spinel in the Tenham meteorite, Nature 221 (1969) 943–944.
[3] A. Putnis, G.D. Price, High-pressure $(Mg, Fe)_2SiO_4$ phases in the Tenham chondritic meteorite, Nature 280 (1979) 217–218.
[4] T.G. Sharp, C.M. Lingemann, C. Dupas, D. Stöffler, Natural occurrence of $MgSiO_3$-ilmenite and evidence for $MgSiO_3$-perovskite in a shocked L chondrite, Science 277 (1997) 352–355.
[5] N. Tomioka, K. Fujino, Natural (Mg, Fe)SiO_3-ilmenite and -perovskite in the Tenham meteorite, Science 277 (1997) 1084–1086.
[6] P. Gillet, M. Chen, L. Dubrovinsky, A. El Goresy, Natural $NaAlSi_3O_8$-hollandite in the shocked Sixiangkou meteorite, Science 287 (2000) 1633–1636.
[7] N. Tomioka, H. Mori, K. Fujino, Shock-induced transition of $NaAlSi_3O_8$ feldspar into a hollandite structure in a L6 chondrite, Geophys. Res. Lett. 27 (2000) 3997–4000.
[8] Z. Xie, N. Tomioka, T.G. Sharp, Natural occurrence of Fe_2SiO_4-spinel in the shocked Umbarger L6 chondrite, Am. Mineral. 87 (2002) 1257–1260.
[9] M. Madon, J.P. Poirier, Dislocations in spinel and garnet high pressure polymorphs of olivine and pyroxene: implications for mantle rheology, Science 207 (1979) 66–68.
[10] G.D. Price, The nature and significance of stacking faults in wadsleyite, natural β-$(Mg, Fe)_2SiO_4$ from the Peace River meteorite, Phys. Earth Planet. Inter. 33 (1983) 137–147.

[11] T.G. Sharp, A. El Goresy, B. Wopenka, M. Chen, A post-stishovite SiO_2 polymorph in the meteorite Shergotty: Implications for impact events, Science 284 (1999) 1511–1513.
[12] V. Malavergne, F. Guyot, K. Benzerara, I. Martinez, Description of new shock-induced phases in the Shergotty, Zagami, Nakhla and Chassigny meteorites, Meteorit. Planet. Sci. 36 (2001) 1297–1305.
[13] K. Oguri, N. Funamori, F. Sakai, T. Kondo, T. Uchida, T. Yagi, High-pressure and high-temperature phase relations in diopside $CaMgSi_2O_6$, Phys. Earth Planet. Inter. 104 (1997) 363–370.
[14] D. Stöffler, K. Keil, E.R.D. Scott, Shock metamorphism of ordinary chondrites, Geochim. Cosmochim. Acta 55 (1991) 3845–3867.
[15] M. Kimura, A. Suzuki, T. Kondo, E. Ohtani, A. El Goresy, Natural occurrence of high-pressure phases jadeite, hollandite, wadsleyite, and majorite-pyrope garnet in an H chondrite, Yamato 75100, Meteorit. Planet. Sci. 35 (2000) A87–A88.
[16] K. Fujino, N. Miyajima, T. Yagi, T. Kondo, N. Funamori, Analytical electron microscopy of the garnet-perovskite transformation in a laser-heated diamond anvil cell, in: M.H. Manghnani, T. Yagi (Eds.), Properties of Earth and Planetary Materials at High Pressure and Temperature, American Geophysical Union, Washington, DC, 1998, pp. 409–417.
[17] M. Chen, T.G. Sharp, A. El Goresy, B. Wopenka, X. Xie, The majorite-pyrope+magnesiowüstite assemblage: Constraints on the history of shock veins in chondrites, Science 271 (1996) 1570–1573.
[18] N. Tomioka, K. Fujino, E. Ito, T. Katsura, T. Sharp, T. Kato, Microstructures and structural phase transition in (Mg, Fe)SiO_3 majorite, Eur. J. Mineral. 14 (2002) 7–14.
[19] R.J. Angel, L.W. Finger, R.M. Hazen, M. Kanzaki, D.J. Weidner, R.C. Liebermann, D.R. Veblen, Structure and twinning of single-crystal $MgSiO_3$ garnet synthesized at 17 GPa and 1800°C, Am. Mineral. 74 (1989) 509–512.
[20] Y. Wang, T. Gasparik, R.C. Liebermann, Modulated microstructure in synthetic majorite, Am. Mineral. 78 (1993) 1165–1173.
[21] S. Heinemann, T.G. Sharp, F. Seifert, D.C. Rubie, The cubic-tetragonal phase transition in the system majorite ($Mg_4Si_4O_{12}$)-pyrope ($Mg_3Al_2Si_3O_{12}$), and garnet symmetry in the Earth's transition zone, Phys. Chem. Miner. 24 (1997) 206–221.
[22] J.B. Brady, R.H. McCallister, Diffusion data for clinopyroxenes from homogenization and self-diffusion experiments, Am. Mineral. 68 (1983) 95–105.
[23] J. Ganguly, V. Tazzoli, Fe^{2+}-Mg interdiffusion in orthopyroxene: Retrieval from the data on intracrystalline exchange reaction, Am. Mineral. 79 (1994) 930–937.
[24] C.S. Schwandt, R.T. Cygan, H.R. Westrich, Magnesium self-diffusion in orthoenstatite, Contrib. Mineral. Petrol. 130 (1998) 390–396.
[25] L. Liu, A.E. Ringwood, Synthesis of a perovskite-type polymorph of $CaSiO_3$, Earth Planet. Sci. Lett. 28 (1975) 209–211.
[26] L. Liu, New silicate perovskites, Geophys. Res. Lett. 14 (1987) 1079–1082.
[27] T. Gasparik, Phase relations in the transition zone, J. Geophys. Res. 95 (1990) 15751–15796.
[28] T. Gasparik, Melting experiments on the enstatite-diopside join at 70-244 kbar, including the melting of diopside, Contrib. Mineral. Petrol. 124 (1996) 139–153.
[29] G.D. Price, A. Putnis, S.O. Agrell, Electron petrography of shock-produced veins in the Tenham chondrite, Contrib. Mineral. Petrol. 71 (1979) 211–218.
[30] V. Voegelé, P. Cordier, F. Langenhorst, S. Heinemann, Dislocations in meteoritic and synthetic majorite garnets, Eur. J. Mineral. 12 (2000) 695–702.
[31] D.M. Hatch, S. Ghose, Symmetry analysis of the phase transition and twinning in $MgSiO_3$ garnet: Implications to mantle mineralogy, Am. Mineral. 74 (1989) 1221–1224.
[32] F. Langenhorst, J.P. Poirier, Anatomy of black veins in Zagami: clues to the formation of high-pressure phases, Earth Planet. Sci. Lett. 184 (2000) 37–55.
[33] C.B. Agee, J. Li, M.C. Shannon, S. Circone, Pressure-temperature phase diagram for the Allende meteorite, J. Geophys. Res. 100 (1995) 17725–17740.
[34] N. Tomioka, K. Fujino, Akimotoite, (Mg, Fe)SiO_3, a new silicate mineral of the ilmenite group in the Tenham chondrite, Am. Mineral. 84 (1999) 267–271.